

High-Frequency Rapid Geo-acoustic Characterization

Kevin D. Heaney

Lockheed-Martin ORINCON Corporation, 4350 N. Fairfax Dr., Arlington VA 22203

Abstract. The Rapid Geo-acoustic Characterization (RGC) algorithm was developed to perform geo-acoustic characterization using the interference patterns of surface ships of opportunity in shallow water. It has been applied successfully at low frequencies to synthetic inversion workshop data and at sea in near real-time. The RGC algorithm determines an effective sediment, which matches the slope (waveguide invariant) and spacing (reciprocal of the time-spread) of interference patterns as well as the fall off in range of the received level. In this paper, we evaluate the extension of the algorithm to mid and high-frequency acoustic signals in shallow water. The issues explored are the robustness of the waveguide invariant, time-spread and TL slope at frequencies above 2 kHz. The algorithm will be applied to a synthetic data example with a known bottom in a range-independent environment.

INTRODUCTION

An approach has been developed to generate effective geo-acoustic parameters using the received low frequency ($f < 800\text{Hz}$) acoustic energy from passing surface ships of opportunity. The Rapid Geo-acoustic Characterization (RGC) algorithm uses a set of acoustic observables to compare pre-computed predictions with the measured data. The pre-computation of these observables from a reduced set of sediment parameters provides the near real-time (after the data has been taken) performance. The RGC has been applied to range-dependent inversion workshop data[1, 2], surface ship of opportunity data[3] and active receptions from a seismic survey transmission[4]. The RGC has been used for low frequency acoustics because of the focus on geo-acoustic parameters, surface ship noise as sources, and low frequency bottom loss model upgrades. This paper is an exploration into the utility of the RGC algorithm for higher frequencies (2-6 kHz).

The first issue is the presence of striations at mid to high frequencies. There is no particular reason to presume that striations would not exist, given the coherent interaction of a finite number of acoustic paths, yet at the higher frequencies the fields are known to exhibit much finer scale structure. We begin this paper by looking at some measured data taken by the NATO Undersea Research Centre during their BOUNDARY 2003 experiment. In Fig. 1, the spectrogram for a passing surface ship is shown from 0 to 1500 Hz. The top panel is the broadband Bearing Time Record (BTR). The ship that is being tracked passes from 90 degrees at the beginning of the data, through end-fire CPA at 19:00. The Scissorgram (beam-steered spectrogram) is

shown in the bottom panel. The striations are clear out to a range of 6 km and up to a frequency of 1200 Hz.

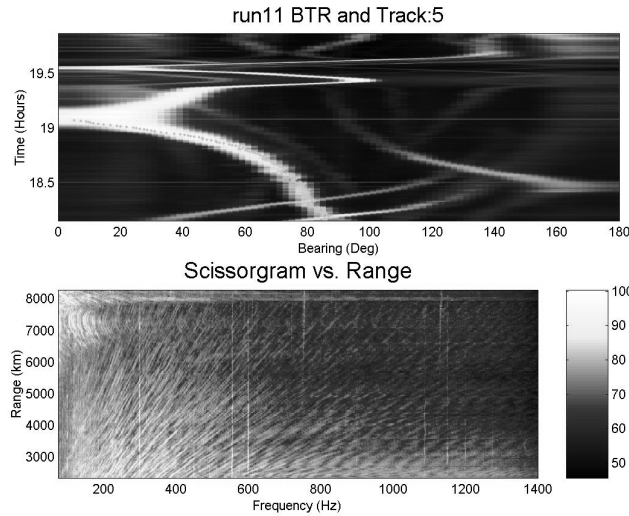


FIGURE 1. At sea measurements during BOUNDARY 2003 of low and mid-frequency striations.

This paper is organized as follows. In section 2 the RGC algorithm is presented. The issue of whether we can use the low frequency acoustic observables at higher frequencies is then examined. The final section involves the application of the RGC to simulated data for a simple sediment model using the frequency band from 4 to 6 kHz.

THE RAPID GEO-ACOUSTIC CHARACTERIZATION ALGORITHM

Striation Slope – Waveguide Invariant (β)

The persistent feature of striations in a shallow-water waveguide has a concise theoretical explanation. The "waveguide invariant" β , was introduced in the Russian literature and is presented in Brekhovskikh and Lysanov[5]. We present a heuristic argument looking at scales of variation in the range/wavenumber and time/frequency domain.

We begin by looking at the dominant oscillations in the intensity of the field as a function of range, at a fixed frequency. Following the Fourier transform analogy, the minimum spacing in range is related to the maximum spread in horizontal wavenumber

$$\Delta r_{\min} \approx \frac{2p}{\Delta k_{\max}} = \frac{2p}{(k_{\max} - k_{\min})} = -\frac{1}{f} \left(\frac{1}{c_{p0}} - \frac{1}{c_{p\max}} \right)^{-1} \quad (1)$$

where the wavenumber has been written as the frequency divided by the phase velocity (c_p).

The time spread is the reciprocal of the minimum frequency spacing of striations, measured from consecutive peaks in the striation pattern at a specific range:

$$t = r \left(\frac{1}{v_{g0}} - \frac{1}{v_{g \max}} \right) \approx \frac{1}{\Delta f_{\min}} \quad (2)$$

where the travel time has been written as the range (r) divided by the group velocity (v_g). The normalized slope is the ratio of the frequency spacing divided by the frequency, to the range spacing divided by the range. Taking the ratio of (1) divided by r and the reciprocal of (2) divided by f yields:

$$\frac{\Delta f / f}{\Delta r / r} = - \frac{\left(\frac{1}{c_{p0}} - \frac{1}{c_{p \max}} \right)}{\left(\frac{1}{v_{g0}} - \frac{1}{v_{g \max}} \right)} = \mathbf{b} \quad (3)$$

where \mathbf{b} is the waveguide invariant, or normalized slope. For environments that are dominated by surface-reflecting, bottom-reflecting (SRBR) ray paths, the waveguide invariant is nearly one for any choice of rays or modes; hence, the name invariant. In the Pekeris waveguide, $\mathbf{b} = \cos^2 \mathbf{q}_{critical}$, which is nearly one. In shallow-water waveguides with more complex sediments, the waveguide invariant varies with the geo-acoustic parameters of the sediment and the water depth[6].

Time Spread (τ)

Having used the slope of the striations as the first observable, there is freedom to choose either the spacing in range or in frequency as the second. The time spread (\mathbf{t}) (Eq. 2) is chosen as the second acoustic observable rather than the wavenumber spacing, because of its relative ease of physical interpretation.

TL slope (\mathbf{a})

The third acoustic observable is the slope of the incoherent TL as a function of range. This parameter is used rather than the absolute TL, to remove the requirement of knowing the source signature. For many shallow-water environments, the Transmission Loss (either band-averaged, or incoherent) can be written as[7]:

$$TL(r) = A + B \log(r) - \mathbf{a}r \quad (4)$$

At ranges beyond several water depths, the high angle propagation will be attenuated and this simple empirical fit to the TL (in dB) will be valid. Cylindrical spreading is assumed ($B = 10$) and the attenuation observable, \mathbf{a} , is defined as the coefficient to a linear fit of the band-averaged TL curve after taking out the cylindrical

spreading. The units of TL and A are dB, r is in kilometers, and \mathbf{a} is in dB/km. In this way, it can be shown that \mathbf{a} is directly related to an average of the modal attenuation (measured in dB/km).

Sediment Model

To facilitate the rapid search of a large parameter space, a simplified sediment model is used. The model is a single, homogenous unconsolidated sediment layer overlying a hard, reflective basement (half-space). The sediment properties (sound speed, density and attenuation) as a function of depth are determined using a parametric model based on the work of Hamilton[8] and Bachman[9]. The model is written explicitly in Heaney[1]. In the low-frequency RGC, the two search parameters are the sediment thickness and the sediment grain size (or compressional speed at the water-sediment interface). For higher frequencies, we do not expect the sediment thickness to be a factor. A much more significant issue (given the larger relative bandwidth) is the frequency exponent of the sediment attenuation. To this end, we perform a 2-dimensional exhaustive search for the sediment compressional speed (at the interface) and the frequency exponent of attenuation (\mathbf{g}). The equation governing the attenuation coefficient in the sediment is therefore:

$$\mathbf{a}(z) = \mathbf{a}_0(z) \left(\frac{f(\text{Hz})}{1000} \right)^{\mathbf{g}} \quad (5)$$

HIGH FREQUENCY DATA AND ACOUSTIC OBSERVABLE COMPUTATION

We now look at a synthetic data set generated using a range-independent normal mode code. The downward refracting profile is shown in Fig. 2.

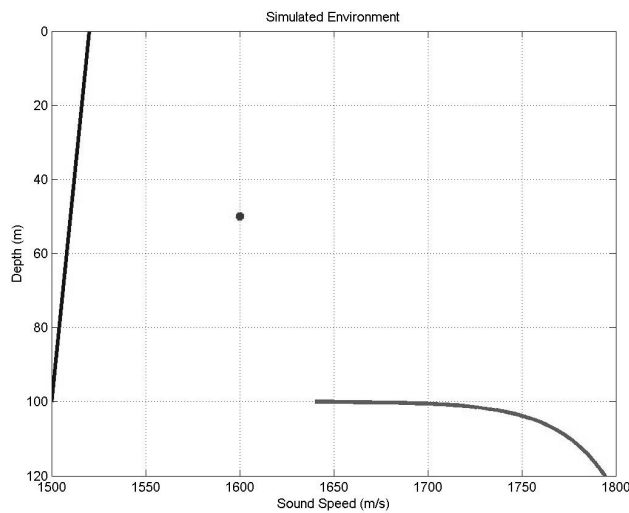


FIGURE 2. Sound speed in the water and sediment for simulations. Source/Receiver depth is 50m.

For this scenario, we model the received signal as if it were from a towed source (at 50 m) to a hydrophone (or beamformed array) at 50 m. The maximum source-receiver range is 3 km, given that we do not expect (because of volume attenuation and source energy spectral levels) to see higher frequencies at longer ranges.

The striation patterns generated from a broadband TL computation are shown in Fig 3. This is a complex pattern exhibiting three distinct interference patterns. The lowest frequency pattern is, we believe, a Lloyds mirror pattern, with a convergence zone at 1800 m. The high frequency oscillations pointing to the upper left (the origin of the plot) correspond to striations with a waveguide invariant value near one. The low frequency oscillations slanting to the upper right correspond to striations with the waveguide invariant value near -3 .

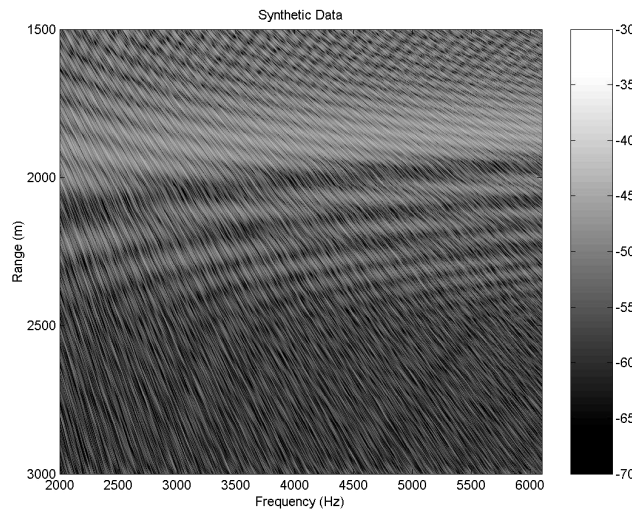


FIGURE 3. Transmission Loss (TL) from a submerged source to a receiver as a function of range/frequency.

Brekhovskikh[5] has shown that for the perfectly reflecting waveguide $\mathbf{b} = 1$ and for the purely refracted case $\mathbf{b} = -3$. This computation demonstrates that striations with $\mathbf{b} = 1$ are visible out to 6 kHz and could, therefore, be used in a geo-acoustic inversion. The high density of striations makes the estimation of the time-spread (reciprocal of the minimum spacing of the dominant striations) difficult so we will utilize a different approach to estimate the time-spread. By computing the autocorrelation of the signal, we can get a (normalized) look at the impulse response of the channel. The results of this computation are shown in Fig. 4.

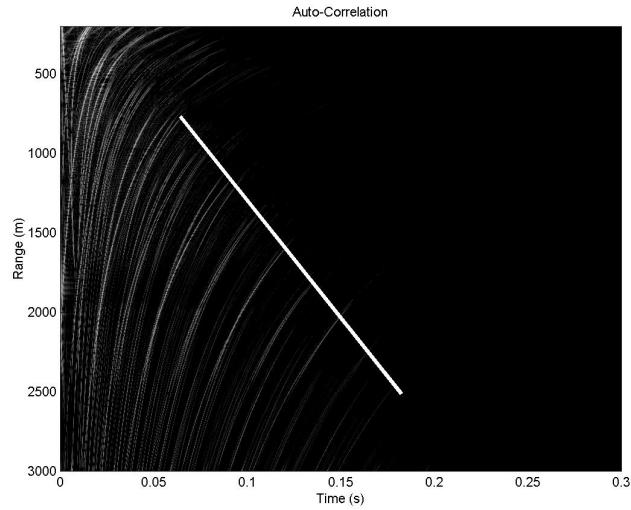


FIGURE 4. Auto-correlation of the signal (corresponding to the spectrum plotted in Fig. 3). The line is hand-drawn to demonstrate the estimation of the time spread as a function of range.

We are now in a position to estimate the acoustic observables for this data-set. The observables are computed at a series of ranges (1000, 1500, 2000, 2500 m) and a frequencies (1000, 2000, 6000 Hz). The waveguide invariant (**β**), the time-spread (**τ**), and the slope of the incoherent (band-averaged) TL vs. range (**α**) is shown in Fig. 5 as a function of range and frequency.

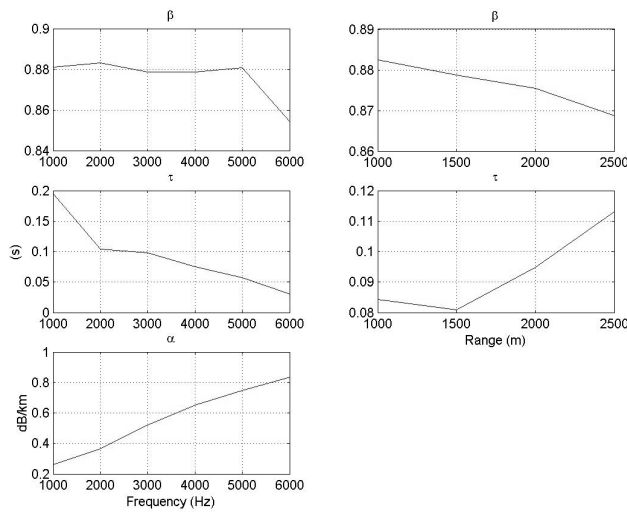


FIGURE 5. Acoustic Observables for simulated dataset. Top panels: waveguide invariant Middle Panels: Time Spread BottomPanel: TL slope

We see that there is a linear change in the waveguide invariant with range. As the propagation range gets larger, higher angles are stripped out and the effective (average) striation slope decreases. The increase in the time-spread with range indicates that dispersion is dominating over mode attenuation (an indication of a hard-

sediment). The TL-slope plot in the lower left indicates that α is a strong function of frequency and is less than 1 dB/km which is also indicative of a hard-sand sediment.

RGC SOLUTION

We now compute determine the RGC solution by computing the acoustic observables for a range of compressional sound speeds at the water-sediment interface (1470 – 1740 m/s) and a range of attenuation coefficients frequency exponents (1 - 2). The approach is quite rapid because we use normal modes at a single frequency to estimate the waveguide invariant (Equation 3), the time-spread and then use the incoherent TL to determine the slope of the TL with range (Equation 5). The full range-dependent model implemented in Heaney[1], used the Parabolic Equation model and required a broadband run for each geo-acoustic estimate. The acoustic observables are computed at each range/frequency for each sediment speed and frequency exponent. The cost function (for each observable) is defined as the RMS error between the predictions and the data over the range/frequency locations of the computation. The results are shown in Fig. 6. For completeness we include using the incoherent TL as a cost function. (This is in the event where the source and receiver are well calibrated.)

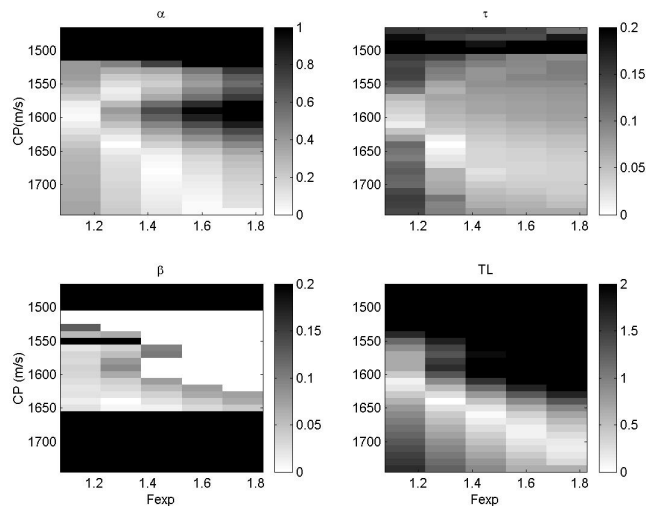


FIGURE 6. Cost functions for the acoustic observables: TL slope, Time-Spread, Waveguide Invariant, and Incoherent TL.

The correct solution (which we are guaranteed to get in this noiseless, simulated example) is with a compressional speed of 1640 m/s and a frequency exponent of 1.3. What is immediately clear from this result is that the correct solution is estimated, but there is degeneracy (ambiguity) between frequency exponent and compressional speed. For the TL inversion in particular (lower-right), sediments with lower

compressional speed and lower frequency exponent have similar TLs than those with higher compressional speeds and higher exponents. The combination of the cost functions does reduce the ambiguity because they have slightly different shapes. The waveguide invariant cost function requires further analysis. It is clear that the numerical code for rapidly estimating the waveguide invariant crashes for high values of compressional speed.

CONCLUSION

We have examined whether the Rapid Geo-acoustic Characterization (RGC) algorithm could be successfully applied at mid to high frequencies. From experimental data and numerical modeling we have seen that stable striations are visible at short ranges for passing surface ships in the 1-6 kHz region. These striations do contain information about the geo-acoustics of the region. A synthetic case was run, and it was demonstrated that the acoustic observables (striation slope, striation spacing, and slope of the incoherent TL vs. range) could be used to successfully invert for the geo-acoustic parameters.

ACKNOWLEDGMENTS

This work was sponsored by SPAWAR and the SBIR office, under the GAIT (Geo-Acoustic Inversion Toolbox) contract. The BOUNDARY 2003 test was conducted by NATO's SACLANT Centre for Undersea Research, with Peter N. Nielsen acting as Senior Scientist.

REFERENCES

1. K. D. Heaney, "Rapid Geoacoustic Characterization: Applied to Range-Dependent Environments," *IEEE Journal of Ocean Engineering*, vol. 29, pp. 43-50, 2004.
2. N. R. Chapman, S. Chinbing, D. King, and R. B. Evans, "Special Issue on Geo-acoustic Inversion In Range-Dependent Shallow-Water Environments," *IEEE Journal of Ocean Engineering*, vol. 28, pp. 317-319, 2003.
3. K. D. Heaney, "Rapid Geoacoustic Characterization Using a Ship of Opportunity," *IEEE Journal of Ocean Engineering*, vol. 29, pp. 88-99, 2004.
4. K. D. Heaney, D. D. Sternlicht, A. Teranishi, B. Castille, and M. Hamilton, "Active Rapid Geoacoustic Characterization using a Seismic Survey Source," *IEEE Journal of Ocean Engineering*, vol. 29, pp. 100-109, 2004.
5. L. M. Brekhovskikh and Y. P. Lysanov, in *Fundamentals of Ocean Acoustics*, 2nd ed. New York: Springer-Verlag, 1991, pp. 140-145.
6. G. L. D'Spain and W. A. Kuperman, "Application of waveguide invariants to analysis of spectrograms from shallow water environments that vary in range and azimuth," *Journal of the Acoustical Society of America*, vol. 106, pp. 2454-2470, 1999.
7. R. J. Urick, *Principles of Underwater Sound for Engineers*. New York: McGraw-Hill Book Company, 1967.
8. E. L. Hamilton, "Geoacoustic Modeling of the Seafloor," *Journal of the Acoustical Society of America*, vol. 68, 1980.
9. R. T. Bachman, "Parameterization of Geoacoustic Properties," 1989.